Asian Journal of Chemistry; Vol. 27, No. 4 (2015), 1251-1256

ASIAN JOURNAL OF CHEMISTRY

http://dx.doi.org/10.14233/ajchem.2015.17472

Effect of H_2O_2 on Corrosion Process of Low Alloy Steel in 3.5 wt. % NaCl Solution

BINGBING ZHAO[1,2], RUILING JIA[1], HUIXIA ZHANG[2,*] and WEIMIN GUO[2]

[1]Inner Mongolia University of Technology, Key Laboratory for Superlight Materials of Inner Mongolia, Huhhot 010051, P.R. China
[2]State Key Laboratory for Marine Corrosion and Protection; Luoyang Ship Material Research Institute, 149 Zhuzhou Road, Qingdao 266101, P.R. China

*Corresponding author: Fax: +86 532 68725001; Tel: +86 532 68725116; E-mail: crystalabx@163.com

Received: 25 February 2014; *Accepted*: 2 June 2014; *Published online*: 4 February 2015; AJC-16769

Corrosion process of low-alloy steel in 3.5 wt. % NaCl solution containing H_2O_2 is studied by cyclic voltammetry curves, cathodic polarization curves, electrochemical impedance spectroscopy and surface characterization analysis. Cyclic voltammetry curves show the addition of H_2O_2 can make the corrosion current of steel increase and corrosion products perform similarly. Cathodic polarization curves confirm that corrosion process is controlled by oxygen diffusion process. Hydrogen peroxide can clearly accelerate the oxygen reduction of low-alloy steel mainly due to the increase of oxygen from decomposition. The electrochemical impedance spectroscopy measurements indicate that the corrosion resistance declines sharply. Surface characterization demonstrates that H_2O_2 can accelerate the corrosion rate, since the pit depth increases by two times in contrast with pure 3.5 wt. % NaCl solutions. These results suggest that the corrosion process of low-alloy steel is similar in 3.5 wt. % NaCl solution with and without H_2O_2, meanwhile the corrosion rate of steels can be efficiently accelerated by adding H_2O_2.

Keywords: Low-alloy steel, Corrosion acceleration, Electrochemical, H_2O_2.

INTRODUCTION

Low-alloy steel, widely used in ships and marine engineering structures, is prone to be corroded in the harsh marine environment. Therefore, the corrosion behaviour of low-alloy steel in seawater needs to be investigated before material selection and engineering design, so that the as-made constructions will be safe and reliable. Currently, to study corrosion behaviour of low-alloy steel, long-term field exposure in natural seawater and short-time laboratory exposures in natural or artificial seawater are used and evaluations of corrosion rate are carried out by corrosion mass loss. The advantages of long-term field exposure are simple operation, real environment, good accuracy and reliability of data. However, test period time is too long, at least one year, typically two to eight years. Yet poor reproducibility because of uncontrolled environment problems makes some data uncertain. And the long test period cannot meet the requirements of rapid development of novel material. Therefore various indoor accelerated tests are devised. For instance, test device for simulating flowing seawater is designed to study the corrosion behaviour of low-alloy steel and the corrosion rate increases by oxygen transfer due to flowing seawater[1]. The alternation of drying and wetting test and natural salt spray test are generally applicable to estimate the tidal corrosion resistance and atmospheric corrosion resistance respectively[2-8]. Whereas, there are few studies related to accelerated test for submerged zone corrosion so far.

In previous works[9,10], different depolarizers were added into 3.5 wt. % NaCl solution to accelerate the submerged zone corrosion process of low-alloy steel. The results illustrated that the test period was shortened by adding H_2O_2 and the relativity and the reproducibility is satisfactory simultaneously. Finally, a new method for estimating the corrosion resistance of low-alloy steel is established by adding H_2O_2 into natural saline solution or seawater[9]. Subsequently, preliminary studies on effect of H_2O_2 to corrosion process of low-alloy steel are carried out[9] and it is found that the compositions of rust layer are almost identical. Both the oxygen reduction processes of the steel are controlled by the two-electronic reaction in solutions with and without[10] H_2O_2. However, further studies related to H_2O_2 effect on corrosion mechanism of low-alloy steel are necessary. In this paper, cyclic voltammetry, potentiodynamic polarization, electrochemical impedance spectroscopy measurements are carried out in order to examine the electrochemical process. Moreover, *in situ* observation of corrosion morphology is implemented to study the corrosion pits development. And the corrosion mechanism of low-alloy steel in 3.5 wt. % NaCl solution containing H_2O_2 is discussed.

EXPERIMENTAL

Materials and preparation methods: The Ni-Cr low alloy steel plate (24 mm in thickness) was obtained by cold rolling. The chemical composition of the steel is presented in Table-1. The steel plate was machined into small pieces with a size of 10 mm × 10 mm × 10 mm, to which copper wire was welded to ensure electrical contact for electrochemical measurements. Then it was mounted with epoxy resin, leaving an exposure area of 1 cm^2 as working electrode. The working electrode was manually ground up to 1200 grit silicon carbide paper, consequently degreased with acetone and then rinsed with deionized water. Test solution, including 3.5 wt. % NaCl solution with and without 0.5 mol/L H_2O_2, was made up from analytical grade reagents and deionized water.

Electrochemical measurements: The ACM 1680 electrochemical workstation was applied for electrochemical measurements. The conventional three-electrode electrochemical cell was used with a platinum-niobium wire with 5 mm in diameter as counter electrode and a saturated calomel electrode (SCE) as reference electrode. In test solutions, the cathodic polarization and cyclic voltammetry (- 0.3 V to - 1.3 V) were performed at a scan rate of 20 mV/min, while the open circuit potential of working electrode attained the stable value. The electrochemical impedance spectroscopy was measured immediately at open circuit potential with a sinusoidal potential excitation of 10 mV amplitude in the frequency range from 100 to 10 mHz. The electrochemical impedance spectroscopy data were fitted with Zview software using equivalent circuit.

TABLE-1
CHEMICAL COMPOSITION OF TEST SPECIMENS (MASS %)

Element	C	Si	Mn	Ni	Cr	Mo	V	P	S	Fe
Content	0.06	0.17	0.30	2.6	0.90	0.20	0.04	0.015	0.01	Remain

Surface characterization: The early corrosion morphology of low alloy steel was observed by HIROX 3D microscope in 3.5 wt. % NaCl solution with and without H_2O_2. The samples were ground up to 2000 grit silicon carbide paper and then polished with diamond paste, finally cleaned by ultrasonic cleaning apparatus. Corrosion characteristics were recorded after different immersion periods (10, 30, 60 and 120 min).

RESULTS AND DISCUSSION

Cyclic voltammetry: Cyclic voltammetry curves of low alloy steel in N_2-saturated 3.5 wt. % NaCl solution (curve a), N_2-saturated 3.5 wt. % NaCl + 0.05 mol/L H_2O_2 solution (curve b) and O_2-saturated 3.5 wt. % NaCl solutions (curve c) are shown in Fig. 1. Only one cathodic peak (a1) at -1.05 V can be observed from Fig. 1a and it can represent the electrochemical reaction of iron itself, such as reduction of Fe^{3+} and Fe^{2+}, as there is no oxygen reduction in N_2-saturated 3.5 wt. % NaCl solution. Two cathodic peaks (b2 and b3) and an anodic peak (b1) are observed in Fig. 1b. It is found that the broad anodic peak (b1) in the potential range -0.75 to -0.5 V encompasses the active metal dissolution with the formation of Fe^{2+} and Fe^{3+} and the H_2O_2 decomposition with formation of O_2 and H_2O. The broad peak b3 of curve b in the potential range -1.1 to -0.95 V includes the reduction of oxygen from H_2O_2 decomposition and the electrochemical reaction of Fe^{2+} and Fe^{3+} reduction, which makes the current density of reduction peak increase by an order of magnitude compared with peak a1. The current in region b2 increases by two orders of magnitude since the reduction of H_2O_2 and HO_2^- ionized from H_2O_2. However decomposition and ionization of H_2O_2 can quickly occur once H_2O_2 encounters aqueous solution and light, such as reaction 1 and 2. The decomposition products of H_2O_2 can increase the dissolved oxygen and effective oxygen concentration, which is designated as the sum of $[O_2]$ and 1/2 $[H_2O_2]$[11]. It confirms that increased current in peak b3 is due to the reduction of oxygen from H_2O_2. Meanwhile, the ionization products of HO_2^- can also decompose oxygen and OH^-, such as reactions 3 and 4, which promotes the oxygen reduction reaction[10]. So the reductive current in region b3 increases compared with the a1 in the solution without H_2O_2.

$$2\,H_2O_2 \rightarrow O_2\uparrow + 2\,H_2O \quad (1)$$

$$H_2O_2 \rightarrow HO_2^- + H^+ \text{ (ionization)} \quad (2)$$

$$HO_2^- + H_2O + 2e^- \rightarrow 3\,OH^- \quad (3)$$

$$2\,HO_2^- \rightarrow O_2\uparrow + OH^- \quad (4)$$

As H_2O_2 can also be considered as an oxidant, reduction of steel and its rusts, *e.g.*, Fe $(OH)_2$, simultaneously occur in region peak b2.

$$H_2O_2 + Fe \rightarrow Fe(OH)_2\downarrow \quad (5)$$

$$H_2O_2 + 2Fe\,(OH)_2 \rightarrow 2Fe(OH)_3\downarrow \quad (6)$$

Fig. 1c shows that an indistinct anodic peak c1 and a distinct cathodic peak c2, which have the same potential region with b1 and b3, respectively. However, a significant decrease in current density of peak c2 comparing with curve a, which illustrates that oxygen reduction reaction takes place in this process. However the reduction current in peak b3 and c2 are equal, while the oxidation current in peak b1 is equal to that of peak c1. Furthermore, an extra shallow peak b2 which represents reduction of hydrogen peroxide and HO_2^- is observed. The above show that the redox current increases in 3.5 wt. % NaCl solution with H_2O_2. These studies prove that the corrosion current of steel increases by adding H_2O_2 and corrosion products are similar.

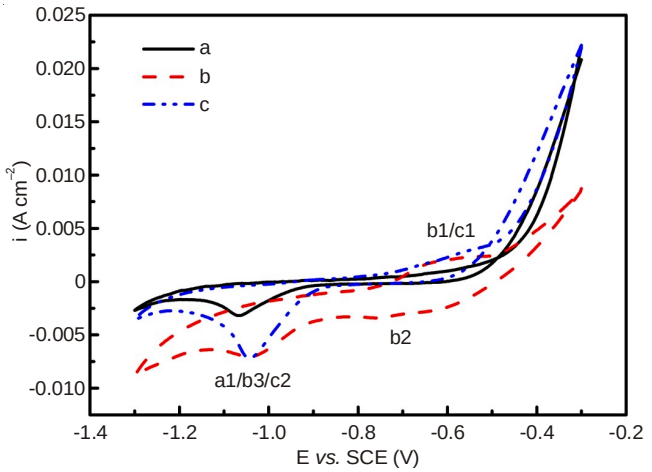

Fig. 1. Cyclic voltammetry curves of low alloy steel: (a) N_2-saturated 3.5 wt. % NaCl; (b) N_2-saturated 3.5 wt. % NaCl + 0.05 mol/L H_2O_2; (c) O_2-saturated 3.5 wt. % NaCl

Cathodic polarization analysis: Fig. 2 shows that polarization curves of low alloy steel in 3.5 wt. % NaCl solution with and without H_2O_2. In 3.5 wt. % NaCl solution, cathodic process undergoes three steps, as shown in Fig. 2a. In region 1, corrosion process is controlled by oxygen ionization reaction. Due to concentration polarization, in region 2, -750 to -960 mV, the corrosion process is mainly controlled by oxygen diffusion. When potential shifts negatively to equilibrium potential of hydrogen electrode, hydrogen depolarization occurs on the metal electrode, as shown in region 3. In the region 3, cathode current density is from the contribution of the reduction current density of oxygen depolarization and hydrogen depolarization. Fig. 2b shows that the polarization curve of low alloy steel in 3.5 wt. % NaCl solution with H_2O_2 and three steps can be observed as the same with Fig. 2a. In contrast to curve a, the corrosion potential shifts to the positive direction about 150 mV and the potential region in step 2 turns broad, over the range -640 to -1200 mV. In this region, the slop of polarization curve is near to vertical. It illustrates that the corrosion process is completely controlled by oxygen diffusion over the potential range -640 to -1200 mV in 3.5 wt. % NaCl solution with H_2O_2. Moreover, the rust layer appears immediately on electrode surface once H_2O_2 is added into the solution and thereby the transfer of oxygen, H_2O_2 and HO_2^- is slow down. As long as the species arrives at the electrode surface, they will immediately be consumed as the result of the reduction reaction. Thus the reduction reaction is suppressed since oxidant encounters scarcity. Thereby the diffusion step of oxygen, H_2O_2 and HO_2^- controls the corrosion process successfully. Meanwhile, the free corrosion current density increases by 2 orders of magnitude comparing with curve a, as H_2O_2 and HO_2^- also contribute to the corrosion current besides oxygen.

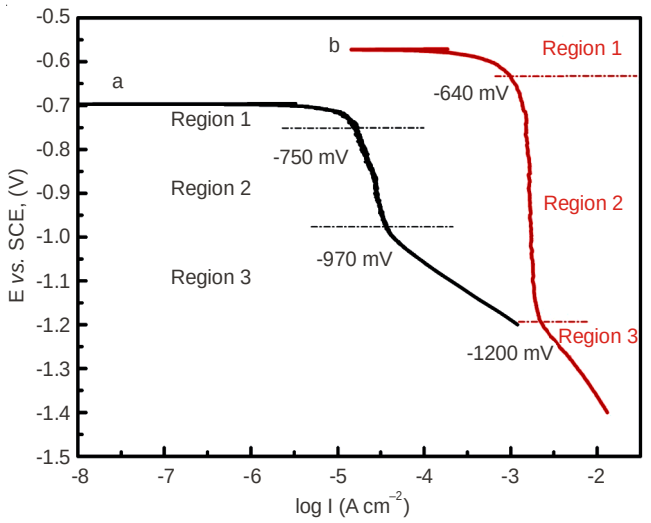

Fig. 2. Polarization curves of low alloy steel in (a) 3.5 wt. % NaCl solution and (b) 3.5 wt. % NaCl solution containing 0.05 mol/L H_2O_2

Evolution of impedance spectra: Fig. 3 shows the Nyquist and Bode plots of low alloy steel immersing in 3.5 wt. % NaCl solution for different immersion times and the Bode plots show that the absolute value of the impedance keeps unaltered with longer immersed time. Furthermore, only one remarkable phase angle peak is observed in Bode plots during the low frequency 1-10 Hz. It illustrates that there is only one time constant, which accounts for the charge transfer processes in the solution/steel interface. Moreover, after immersion for 8 h, all the shape of nyquist plots at low frequency is near to a line, whose slop is slightly smaller than 45° due to dispersion effect. It shows that the corrosion process is controlled by oxygen diffusion after immersing for 8 h. Therefore, the equivalent

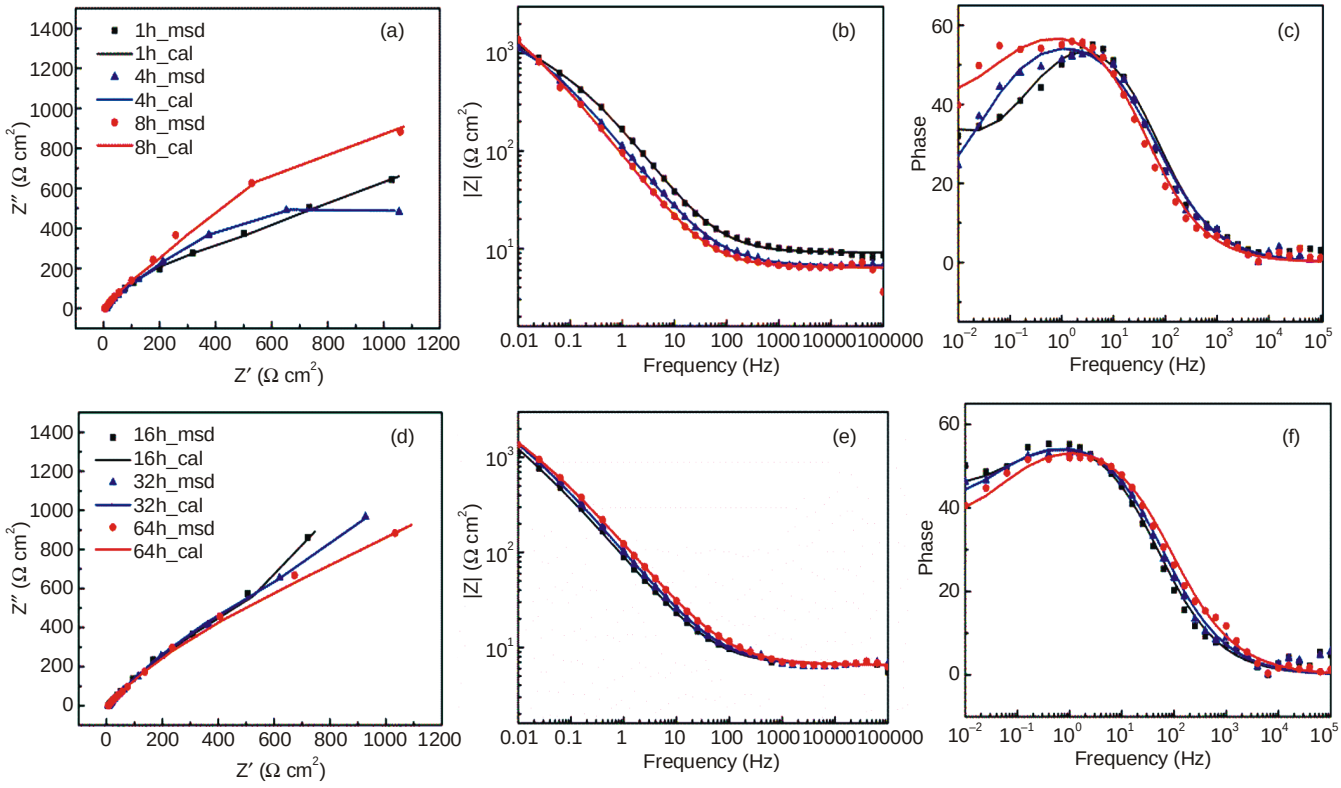

Fig. 3. EIS plots in 3.5 wt. % NaCl solution after immersing for; (a) 1 h (b) 4h (c) 8 h (d) 16 h (e) 32 h (f) 64 h

electric circuit a,b given in Fig. 5 is, respectively adequate to describe the measured EIS spectra in Fig. 3. In this circuit, R_s is the resistance of the solutions, Q is the constant phase element (CPE) which represents the capacitance of the double layers and R_t is the charge transfer resistance. Z_w is Warburg impedance which represents the influence of concentration polarization and elemental diffusion on the electrode reaction which only exists at low frequencies.

However, two and half remarked phase angle peaks are observed in Bode plots of low alloy steel immersing in 3.5 wt. % NaCl solution with H_2O_2 for 1, 4, 8 and 16 h and it shows that there are three time constants in the corrosion process. The first one at high frequency is related to the process of the outer loose rusty layer, while the second one at middle frequency and the last one at low frequency respectively accounts for the process of barrier layer and corrosion process at the barrier layer/metal interface. Therefore, the equivalent electric circuit in Fig. 6a is proposed to explain the measured EIS spectra in Fig. 4a, b and c. In this circuit, Q_l and Q_b are the CPEs which respectively represent the capacitances of the loose and barrier rust layer, while R_l and R_b are, respectively the resistance of the loose and barrier rust layer. R_t is the charge transfer resistance. C_{cd} is the double layer capacitance and Z_o is the diffusion impedance of finite layer. Z_o represents the influence of concentration polarization and elemental diffusion on the electrode reaction. After immersion for 32 h, the half phase peak disappears and two remarked phase angle peaks shift to higher frequency, as shown in Fig. 4d, e and f. At this moment, there are two time constants in corrosion process, so that the circuit without Q_l and R_l is given in Fig. 6b to describe the measured EIS spectra in Fig. 4d, e and f.

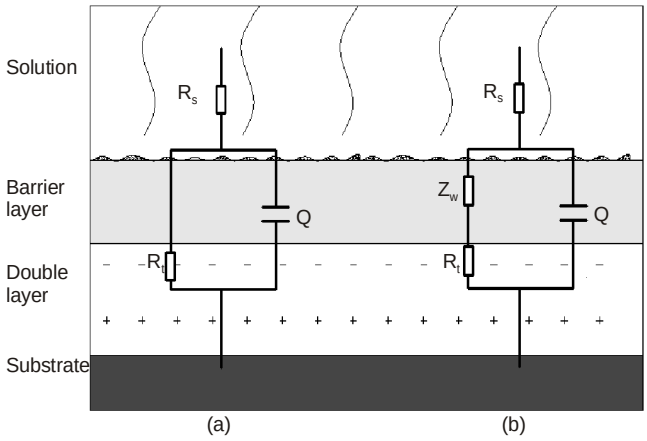

Fig. 5. Equivalent circuit for low alloy steel in 3.5 % NaCl

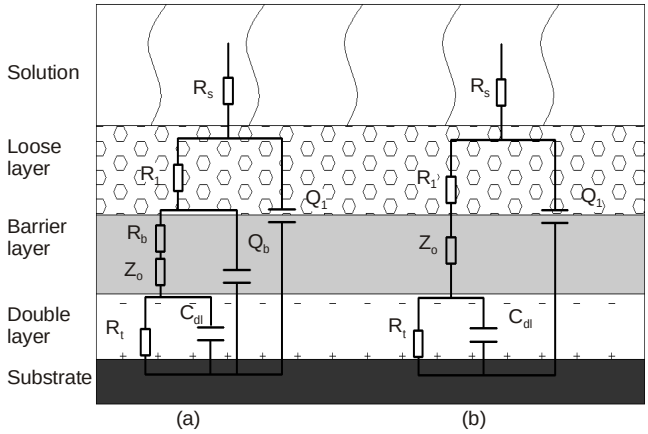

Fig. 6. Equivalent circuit for low alloy steel in 3.5 % NaCl + 0.05 mol/L H_2O_2

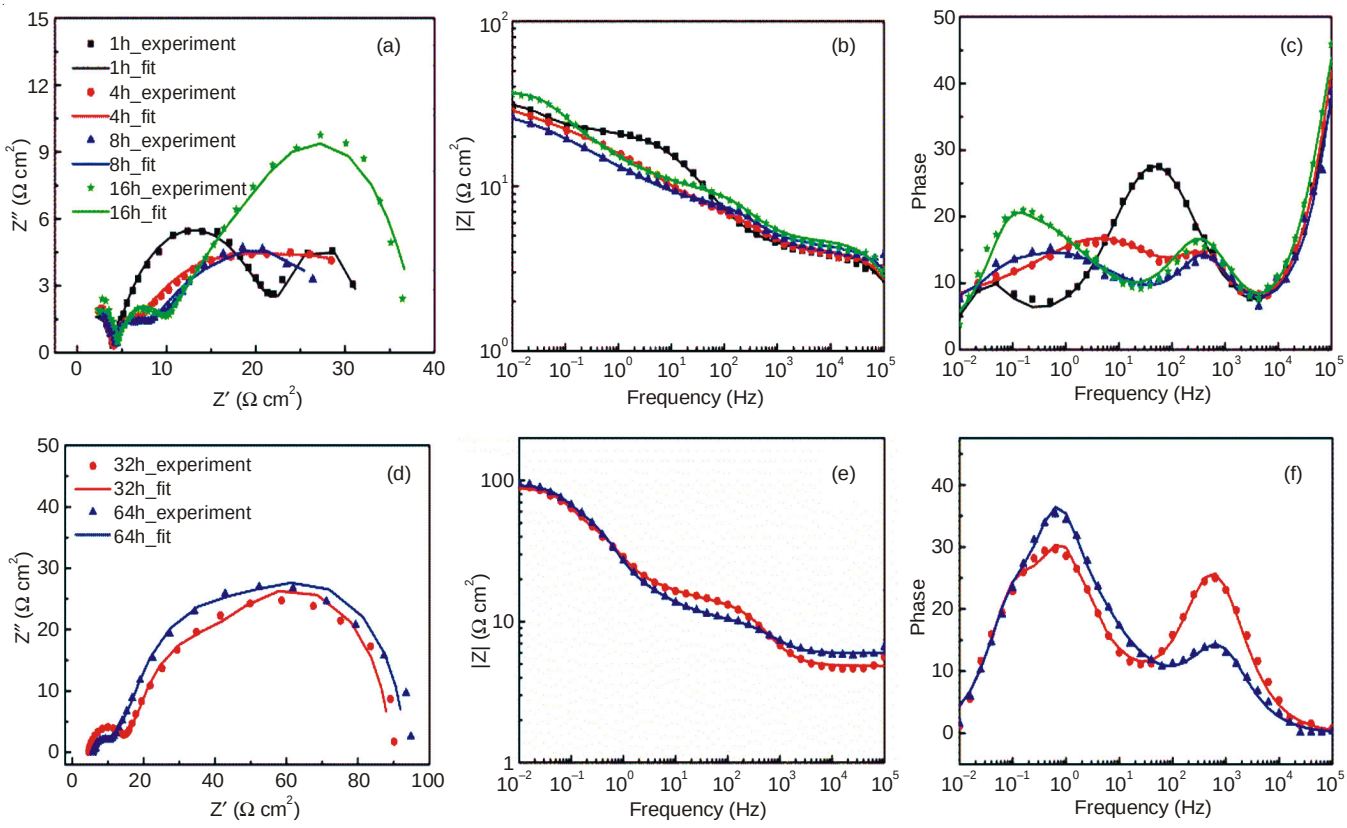

Fig. 4. EIS plots in 3.5 wt. % NaCl solution containing H_2O_2 for (a) 1 h, (b) 4 h (c) 8 h (d) 16 h (e) 32 h (f) 64 h

The fitted results are shown in Fig. 7 and it is obvious that R_t of sample in 3.5 % NaCl solution containing H_2O_2 is 2 orders of magnitude lower than that in 3.5 % NaCl solution and it is proved that instantaneous corrosion rate increases because of H_2O_2. Furthermore it can be observed that the loose rust layer is falling off from the sample surface in the solution containing H_2O_2 in the whole corrosion process and the black barrier layer which is mainly composed of Fe_3O_4 is uncovered to the solution. Fe_3O_4 can form either directly from Fe or by the conversion of $Fe(OH)_2$. The 3.5 % NaCl solution is near to neutral and $Fe(OH)_2$ film forms rapidly, as shown in the reaction 7, 8 and 9. Moreover, it converts to Fe_2O_3 or Fe_3O_4, as shown in the reaction 10 and 11, in respect that the evolution of corrosion products abides by the principle of thermodynamic stability. Thus the rusty layer on sample surface in 3.5 % NaCl solution is mainly composed of $Fe(OH)_2$, α-FeOOH, α-Fe_2O_3 and Fe_3O_4 and loose layer is made up of $Fe(OH)_2$, α-FeOOH and α-Fe_2O_3, while barrier layer is mainly made[9,10] up of Fe_3O_4. However, the transfer of oxygen from the bulk solution to the metal surface/solution interface is slow down by the rusty layer, so the oxygen diffusion is the lowest step during the electrochemical corrosion process and dominates the corrosion process. The oxygen diffusion can also be examined from the polarization curves in Fig. 2 and EIS plots in Fig. 3.

$$H_2O \rightarrow OH^- + H^+ \quad (7)$$

$$Fe + OH^- \rightarrow [Fe(OH)_{ads} + e] \rightarrow FeOH^+ + 2e \quad (8)$$

$$FeOH^+ + OH^- \rightarrow Fe(OH)_2 \quad (9)$$

$$Fe(OH)_2 \rightarrow \alpha\text{-}FeOOH + H_2\uparrow \rightarrow \alpha\text{-}Fe_2O_3 \quad (10)$$

$$Fe(OH)_2 \leftrightarrow Fe(OH)_3^- \leftrightarrow Fe_3O_4 \quad (11)$$

When adding H_2O_2 into 3.5 wt. % NaCl solution, the decomposition and ionization of H_2O_2, as shown by reactions 1 and 2, make the solution weakly acidic. Simultaneously the dissolved oxygen concentration increases. The hydrogen and oxygen evolutions generate air bubbles, which makes the loose layer to fall off from the barrier layer. Thus Fe_3O_4 layer exposes into the solution with H_2O_2. Compared with the immersion in early period, there are only two constants left after immersion for 32 h. Moreover, it can be observed from the fitted results in Fig. 7 that the R_t values fluctuate in the magnitude of

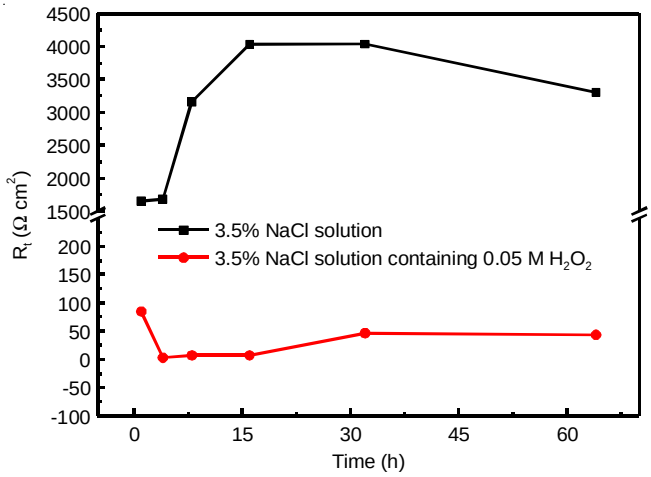

Fig. 7. Evolution of R_t with immersion time

10^3 Ω cm^2 in 3.5 % NaCl solution. Also, it can be found that R_t increases first then decreases after immersion for 32 h, which is two orders of magnitude higher than that in 3.5 % NaCl solution with H_2O_2. And this result keeps consistent with polarization curves of low alloy steel in 3.5 wt. % NaCl solution with and without H_2O_2.

***in situ* Monitoring corrosion characteristic:** It can be seen from Fig. 8 that there is only one obvious pit on limited measurement area of sample surface after immersing for 10, 30, 60 and 120 min. In contrast, there are three, four and five pits appearing in the initial, medium and ultimate periods respectively, as shown in Fig. 9. Moreover, it can be concluded from Table-2 that the longer immersed time, the larger pit angle and depth will be (Pit angle is defined by Fig. 10). It can also be observed that pit is expanding towards its surrounding zone during the immersing period in 3.5 % NaCl solution with and without H_2O_2. And the surrounding zone of pit is covered with rust in 3.5 % NaCl solutions. However, almost all the limited measurement area is covered with rust in the solution with H_2O_2. It is illustrated that corrosion on low alloy steel surface develops more rapidly after adding H_2O_2, which is attributed to not only the increase of dissolved oxygen from decomposition of H_2O_2 but also the reaction of H_2O_2 and steel or corrosion products, *e.g.*, $Fe(OH)_2$, FeOOH, FeO.

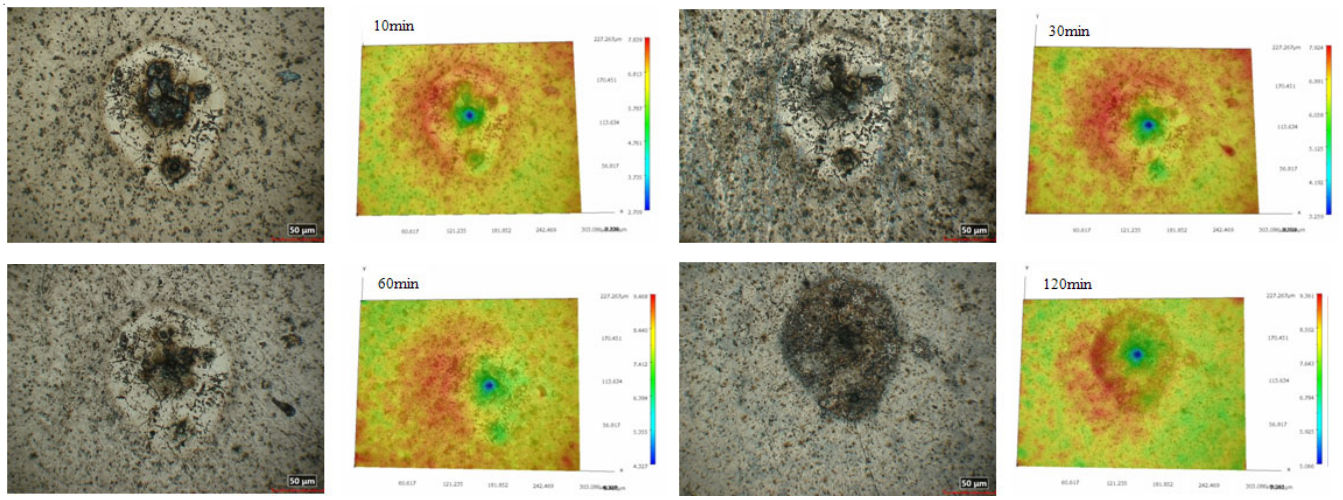

Fig. 8. Corrosion morphology of low-alloy steel in 3.5 % NaCl (× 1000)

TABLE-2
MEASUREMENT RESULTS OF PITTING DEPTH AND ANGLE

Solution	Immersing time (min)	10	30	60	120
3.5 % NaCl	Pit depth (μm)	4.711	4.631	4.785	4.253
	Angle (deg)	15.407	12.148	13.288	14.314
3.5 % NaCl + 0.05 mol/L H_2O_2	Pit depth (μm)	9.025	9.362	10.142	11.382
	Angle (deg)	41.614	43.034	43.577	46.986

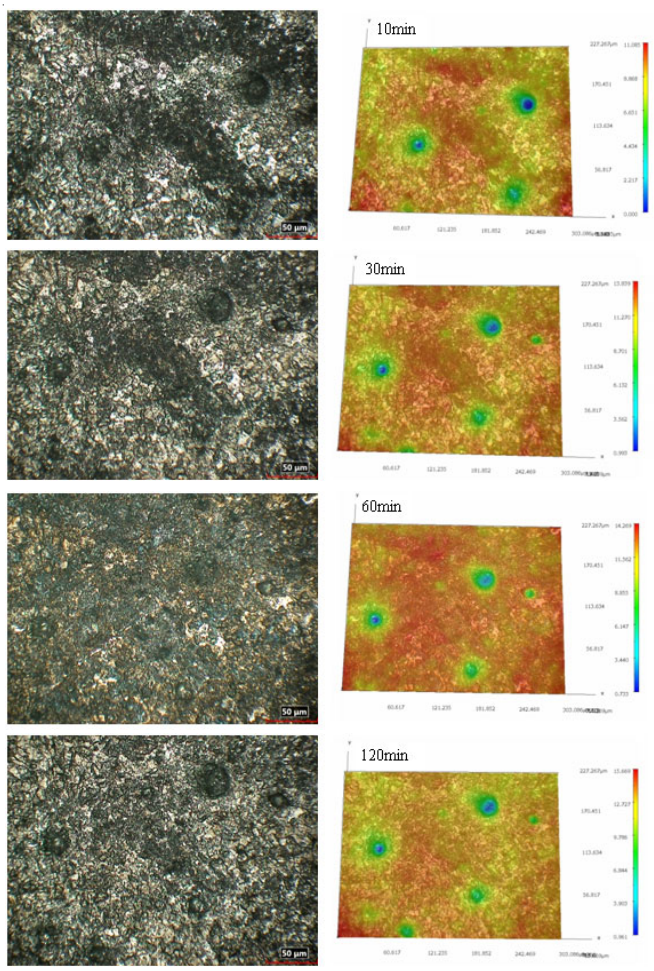

Fig. 9. Corrosion morphology of low-alloy steel in 3.5 % NaCl + 0.05 mol/L H_2O_2 (× 1000)

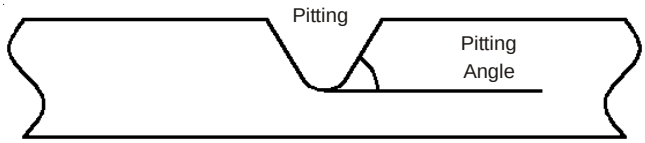

Fig. 10. Calculation method to determine pitting angle

Conclusion

The addition of H_2O_2 will not introduce impurity ions and the forming process of corrosion products is similar to 3.5 % NaCl solutions. The OCP shifts positively and limited diffusion current density increased remarkablely, meanwhile the hydrogen-evolution potential also shifted negatively. The corrosion process is similar in 3.5 % NaCl solutions with and without H_2O_2. H_2O_2 can promote the cathodic reduction because it makes the effective concentration of oxygen increase.

ACKNOWLEDGEMENTS

The authors are grateful to the State Key Laboratory for Marine Corrosion and Protection for the financial support.

REFERENCES

1. W.X. Jin, Y.N. Luo and S.Z. Song, *J. Chinese Soc. Corros. Prot*., **28**, 337 (2008).
2. H. Zhang, H.B. Qi, C.W. Du and X.G. Li, *Acta Metall. Sin.*, **45**, 338 (2009) (in Chinese).
3. A. Nishikata, Y. Yamashita, H. Katayama, T. Tsuru, Usami, K. Tanabe and H. Mabuchi, *Corros. Sci*., **37**, 2059 (1995).
4. A.P. Yadav, A. Nishikata and T. Tsuru, *Corros. Sci*., **46**, 169 (2004).
5. Y.Y. Chen, H.J. Tzeng, L.I. Wei, L.H. Wang, J.C. Oung and H.C. Shih, *Corros. Sci*., **47**, 1001 (2005).
6. Y.Y. Chen, H.J. Tzeng, L.I. Wei and H.C. Shih, *Mater. Sci. Eng. A*, **398**, 47 (2005).
7. T. Nishimura, H. Katayama, K. Noda and T. Kodama, *Corros. Sci*., **42**, 1611 (2000).
8. L. Hao, S. Zhang, J. Dong and W. Ke, *Corros. Sci*., **58**, 175 (2012).
9. H.X. Zhang, X. Qi, H.B. Zeng and C.-L. Deng, *Corros. Sci. Prot. Technol.*, **22**, 192 (2010).
10. C. Yang, H.X. Zhang, W.M. Guo *et al*., *J. Chinese Soc. Corros. Prot*., **33**, 205 (2013).
11. S. Uchida, E. Ibe, K. Nakata, M. Fuse, K. Ohsumi and Y. Takashima, *Nucl. Technol*., **110**, 250 (1995).